



Article

First Occurrence of Titanian Hydroxylclinohumite in Marble-Hosting Gem Spinel Deposits, Luc Yen, Vietnam

Vladimir G. Krivovichev ^{1,*}, Katherine A. Kuksa ², Pavel B. Sokolov ³, Taras L. Panikorovskii ⁴, Vladimir N. Bocharov ⁵ and Geir Atle Gussisås ⁶

¹ Department of Mineralogy, Institute of Earth Sciences, St. Petersburg University, University Embankment, 7/9 (V.G.K.), 199034 St. Petersburg, Russia

² Department of Geomorphology, Institute of Earth Sciences, St. Petersburg University, University Emb. 7/9, 199034 St. Petersburg, Russia; katerina.kuksa@spbu.ru

³ SOKOLOV Co. Ltd., Gatchinskaya str., 11/A, 7N, 197136 St. Petersburg, Russia; pavel.sokolov@gemstone.ru

⁴ Laboratory of Nature-Inspired Technologies and Environmental Safety of the Arctic, Kola Science Centre, Russian Academy of Sciences, 14 Fersman Street, 184200 Apatity, Russia; t.panikorovskii@ksc.ru

⁵ Geo Environmental Centre "Geomodel", the Research Park, St. Petersburg University, Ul'yanovskaya Str. 1, 198504 St. Petersburg, Russia; bocharov@molsp.phys.spbu.ru

⁶ BalderGems Co., Yen The 36000, YB, Vietnam; baldergems@gmail.com

* Correspondence: v.krivovichev@spbu.ru; Tel.: +7-(812)-3289481

Abstract: In this paper, we report the very first occurrence of titanian hydroxylclinohumite in the marble-hosted gem spinel deposits of the Luc Yen district, northern Vietnam. Hydroxylclinohumite is anhedral and associated with forsterite, tremolite, pargasite, diopside, spinel, dolomite and calcite. Hydroxylclinohumite from the Luc Yen deposit was characterized via electron microprobe analysis, single-crystal X-ray diffraction study, and Raman spectrometry. The average composition is $(\text{Mg}_{0.69}\text{Ti}_{0.29}\text{Fe}_{0.02})_{\Sigma 1.00}\text{Mg}_{7.91}(\text{SiO}_4)_{4.08}[(\text{OH})_{1.10}\text{F}_{0.53}\text{O}_{0.37}]_{\Sigma 2.00}$. (ideally $(\text{Mg}_{0.7}\text{Ti}_{0.3})_{\Sigma 1}\text{Mg}_{8.0}(\text{SiO}_4)_4[(\text{OH})_{1.2}\text{F}_{0.5}\text{O}_{0.3}]_2$). The compositions of the analyzed hydroxylclinohumites have a narrow range of Mg/(Mg+Fe+Ti) values (0.96–0.97) and a defined hydroxylclinohumite solid-solution series. Compared with other occurrences, the Luc Yen hydroxylclinohumite has an average titanium content, which attains 0.31 atoms per formula unit (3.93 wt.% TiO_2) and a low iron content of 0.04 atoms per formula unit (0.42 wt.% FeO). The formation of hydroxylclinohumite is favored by the proportion of Mg, and Si in the precursor rocks and the increased activity of H_2O in the fluid phase.

Keywords: titanian hydroxylclinohumite; humite supergroup; Raman spectrum; gem spinel; marble-hosted deposits; analysis of mineral parageneses; Luc Yen district; Vietnam



Citation: Krivovichev, V.G.; Kuksa, K.A.; Sokolov, P.B.; Panikorovskii, T.L.; Bocharov, V.N.; Gussisås, G.A. First Occurrence of Titanian Hydroxylclinohumite in Marble-Hosting Gem Spinel Deposits, Luc Yen, Vietnam. *Minerals* **2023**, *13*, 901. <https://doi.org/10.3390/min13070901>

Academic Editor: Felix Brandt

Received: 8 June 2023

Revised: 23 June 2023

Accepted: 28 June 2023

Published: 2 July 2023



Copyright: © 2023 by the authors. Licensee MDPI, Basel, Switzerland. This article is an open access article distributed under the terms and conditions of the Creative Commons Attribution (CC BY) license (<https://creativecommons.org/licenses/by/4.0/>).

1. Introduction

In the recent literature, considerable attention has been paid to hydroxylclinohumite (ideally $\text{Mg}_9(\text{SiO}_4)_4[(\text{OH})_2]$, the OH-dominant equivalent of clinohumite) as a possible site of water in the upper mantle of the Earth [1–8]. Before its discovery in the Zelentsovskaya mine near Magnitka (Zlatoust district, Southwestern Urals) and approval by the CNMNC MMA as an independent mineral species [9], hydroxylclinohumite has been reported for many decades as an accessory mineral in the rocks of ultrabasic composition including carbonatites, kimberlites, peridotites and serpentinites [1,2,10–15]. It should be noted that magnesian humite group of minerals found in carbonate rocks are reported as typically titanium-poor and fluorine-rich, whereas those in ultrabasic rocks are enriched in titanium and generally contain little or no fluorine [15]. In general, the composition of titanian hydroxylclinohumite can be represented by the formula $(\text{M}_{1-x}\text{Ti}_x)_{\Sigma 1.0}\text{M}_8(\text{SiO}_4)_4[(\text{OH})_{2-2x}\text{O}_{2x}]_{\Sigma 2.0}$, where, M is Mg, Fe^{2+} , Mn and Ni, and x has values up to 0.5 [16–18].

Against the background of a renewed interest in magnesian minerals of the humite group, we present the results of a comprehensive study (chemical composition, Raman

spectroscopy and X-ray data) of the first discovery of titanian hydroxylclinohumite in marbles from the Luc Yen gem spinel deposit, which is located in northern Vietnam in the Yen Bai province. Discovered at the end of the last century [19] and then singled out as an important source of spinel and corundum of jewelry quality [20–22], this deposit immediately attracted the close attention of researchers. The main issues discussed were related to the peculiarities of the chemical composition of spinel [21,23–25], specifically in order to identify the diagnostic signs that make it possible to distinguish Luc Yen spinel entering the jewelry market from the spinels of other deposits. Special studies concern the nature of the spinel coloration [19,26], assessment of the age of the host marbles [27], and the conditions of their formation [28–33]. Most attention has been paid to the geology and genesis of the spinel-containing marbles [24].

Clinohumites have long since been described as being associated with gem spinel in the Cong Troi deposit of Luc Yen [34]. Later, the major element of clinohumite and its stable isotope composition were described briefly in [35] and some petrological constraints were placed on the minimal temperature and fluid composition of a clinohumite-bearing assemblage. Afterwards, Hurai et al. [36] claimed to present the first detailed study of Luc Yen hydroxylclinohumite, but, unfortunately, it appeared not to be hydroxylclinohumite; this was because as a result of refining its crystal structure the formula corresponded to clinohumite ([36]: $(\text{Mg}_{8.95}\text{Ti}_{0.05})(\text{SiO}_4)_4[\text{F}_{1.03}(\text{OH})_{0.97}]_{\Sigma 2.00}$, or, taking into account the presence of titanium (and seeking to preserve electroneutrality), we have: $(\text{Mg}_{8.95}\text{Ti}_{0.05})(\text{SiO}_4)_4[\text{F}_{1.03}(\text{OH})_{0.87}\text{O}_{0.10}]_{\Sigma 2.00}$. Consequently, the refined predominance of fluorine over hydroxide ($\text{F}_{1.03}\text{OH}_{0.87}$) in comparison with the results of electron microprobe analysis ($\approx (\text{OH})_{1.05}\text{F}_{0.95}$) cannot be as a result of measurement inaccuracy, and the matrix effect of EPMA analysis of fluorine [37].

The aim of the current work is to present detailed information on the first occurrence of titanian hydroxylclinohumite in the Luc Yen (Vietnam) marble-hosted deposit of ruby and gem spinel (the first discovery of titanian hydroxylclinohumite in this genetic type of deposits).

2. Geological Setting and Petrography

The primary Luc Yen gem spinel deposit is situated in the Yen Bai province of northern Vietnam. This region comprises two structural zones separated by a fault: the Lo Gam metamorphic zone and the Day Nui Con Voi range [20]. The Lo Gam zone consists predominantly of marbles in which multicolored spinel is disseminated as lenses and “pockets” forming the famous Luc Yen gem deposit [20,38]. In addition to carbonates (calcite, and dolomite) and spinel, the marble units in the Luc Yen deposit contain phlogopite, pargasite, forsterite, clinohumite, preiswerkite [39], pyrite, corundum, dravite, pyrrhotite, and graphite.

According to our previous investigation, only some blue, lavender and purplish spinel is associated with humite minerals [33]. Type 4 blue spinel from Phan Thanh could be found in grey calcitic marbles with abundant graphite and straw-colored chondrodite–norbergite [22]. At the same time, type 1 lavender and purplish spinel from the Cong Troi deposit is often associated with ginger or orange-brown clinohumite, pargasite, and pyrite in dolomite–calcite marble (Figure 1).

Clinohumite is usually presented as orange-brown blebs or subhedral grains of 1–3 mm in size embedded in the dolomite–calcite matrix. Sometimes, it forms aggregates up to 1–3 cm, overgrowing spinel grains, filling its cavities and fissures (Figure 1). Parts of these clinohumites belong to hydroxylclinohumite. Clinohumite often contains the following minerals: calcite, forsterite, pargasite, pyrite, serpentine and rutile (Figure 2).

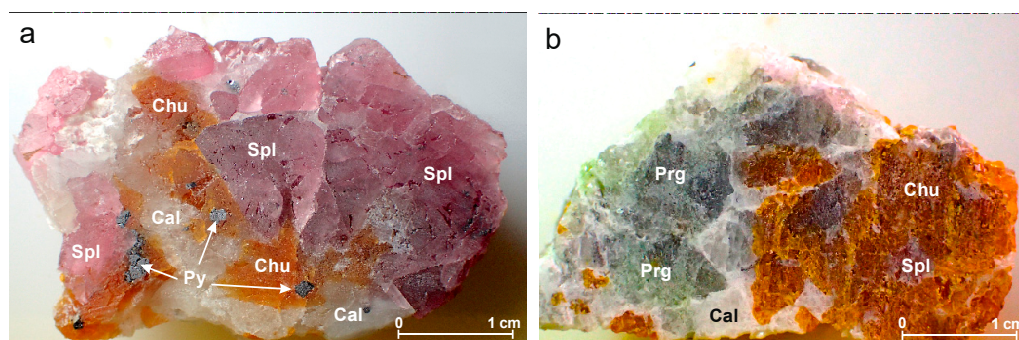


Figure 1. Typical occurrence of clinohumite in the Cong Troi deposit of Luc Yen: (a) subhedral orange clinohumite with pyrite inclusions partially overgrowing purplish gem spinel and filling in fractures and cavities in calcitic marbles; (b) unihedral orange-brown clinohumite overgrowing lavender spinel with green pargasite in dolomitic calcite marble. Mineral symbols: Spl—spinel, Chu—clinohumite, Prg—pargasite, Py—pyrite, Cal—calcite.

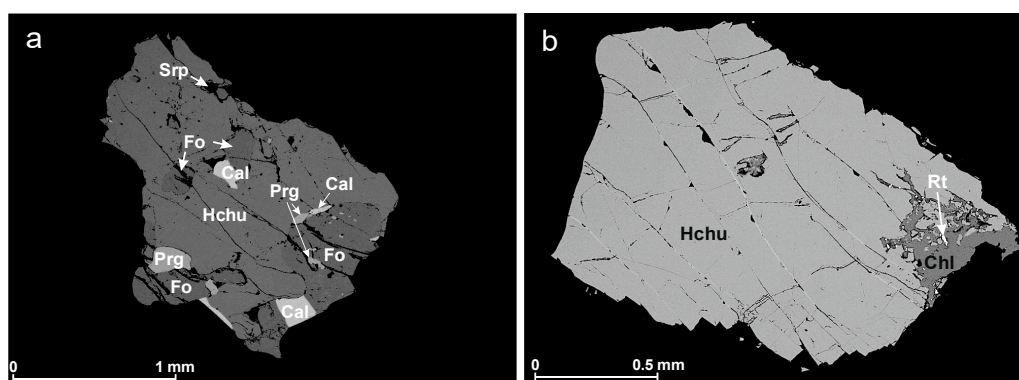


Figure 2. Back-scattered electron microscopy images of a polished section of the Luc Yen hydroxylclinohumite: (a) hydroxylclinohumite with calcite, forsterite, pargasite and serpentine inclusions (sample V-11-2a); (b) hydroxylclinohumite altered from one rim to chlorite (sample V-12-03). Cal—calcite; Hchu—hydroxylclinohumite; Fo—forsterite; Prg—pargasite; Spr—serpentine; Chl—chlorite; Rt—rutile.

3. Materials and Methods

3.1. Microprobe Analysis

Major element compositions of hydroxylclinohumite from thin sections of samples were determined at the Electron Microprobe Laboratory in the Geomodel Center of St. Petersburg University using a JEOL-8200 Electron Microprobe. Natural standards were used for calibration. An operating voltage of 15 kV and a beam current of 20 nA were used with a beam diameter of 1 μm (5 μm spot size). Representative results of the electron microprobe analyses of the Luc Yen hydroxylclinohumite are listed in Table 1.

3.2. Single-Crystal X-ray Diffraction

Single-crystal X-ray diffraction study for samples V-11-2d, V-11-2a and V-12-03 was conducted via a XtaLAB Synergy-S diffractometer (Rigaku corp., Tokyo, Japan) equipped with a hybrid photon counting detector HyPix-6000HE using monochromatic radiation $\text{MoK}\alpha$ ($\lambda = 0.71069\text{\AA}$) at the Centre of the Collective Use of Equipment, Kola Science Centre. More than half of the diffraction sphere was collected with scanning step 1° , and exposure time 0.5–1 s. The data were integrated and corrected via the CrysAlisPro [40] program package, which was also used to apply an empirical absorption correction using spherical harmonics, as implemented in the SCALE3 ABSPACK scaling algorithm. The SHELXL program [41] was used for the crystal structures' refinement. The crystal structures were drawn using the VESTA 3 program [42]. The structures of clinohumite were refined in the

traditional (non-standard) setting $P2_1/b$ in order to emphasize the structural relationship to olivine [43]; $R_1 = 0.027, 0.023$ and 0.025 for the V-11-2d, V-11-2a and V-12-03 samples, respectively. Position of the hydrogen atoms was determined using difference Fourier maps. The SCXRD data are deposited in CCDC (<https://www.ccdc.cam.ac.uk/>, accessed on 23 April 2023) under entries No. 2257900–2257902. Crystal data, data collection information and structure refinement details are given in Table 2; atom coordinates and selected interatomic distances are in Supplementary Tables S1–S6.

Table 1. Results of electron microprobe analyses of hydroxylclinohumite from the Luc Yen deposit.

	V-11-2d	V-11-2a	V-12-03	\bar{X}	σ
SiO ₂ wt%	38.58	38.64	38.91	38.71	0.17
TiO ₂	3.33	3.90	3.93	3.72	0.34
MgO	54.79	54.57	54.63	54.66	0.11
* FeO	0.35	0.42	0.00	0.26	0.22
F	1.85	1.50	1.37	1.57	0.25
** H ₂ O	1.47	1.60	1.61	1.56	0.08
Total	100.41	100.63	100.45	100.50	0.12
-O=F ₂	0.76	0.64	0.58	0.66	0.09
Total	99.65	99.99	99.87	99.84	0.17
*** Si apfu	4.07	4.07	4.10	4.08	0.02
Ti	0.27	0.30	0.31	0.29	0.02
Mg	8.63	8.59	8.59	8.60	0.02
Fe	0.03	0.04	0.00	0.02	0.02
OH	1.04	1.13	1.13	1.10	0.05
F	0.62	0.50	0.46	0.53	0.08
O	0.34	0.37	0.41	0.37	0.03
Mg#	0.97	0.96	0.96	0.96	0.01

* Total Fe as FeO; ** calculated from stoichiometry; *** atomic proportions based on 13 cations; Mg#—Mg/(Mg+Fe+Ti); \bar{X} —arithmetic mean; σ —standard deviation.

Table 2. Crystal data and structure refinement of hydroxylclinohumite from the Luc Yen deposit.

Identification Code	V-11-2d	V-11-2a	V-12-03
Temperature/K		293(2)	
Crystal system		monoclinic	
Space group		$P2_1/b11$	
$a/\text{Å}$	4.7381(2)	4.74060(10)	4.7386(2)
$b/\text{Å}$	10.2423(4)	10.2431(3)	10.2416(3)
$c/\text{Å}$	13.6531(6)	13.6551(4)	13.6597(5)
$\alpha/^\circ$	100.917(4)	100.935(3)	100.905(3)
Volume/ Å^3	650.58(5)	651.03(3)	650.95(4)
Z		2	
$\rho_{\text{calc}}/\text{cm}^3$	3.199	3.197	3.200
μ/mm^{-1}	1.118	1.122	1.135
F(000)	623.0	623.0	624.0
Crystal size/ mm^3	$0.15 \times 0.13 \times 0.1$	$0.22 \times 0.15 \times 0.14$	$0.17 \times 0.12 \times 0.1$
Radiation		Mo K α ($\lambda = 0.71073$)	
2 θ range for data collection/ $^\circ$	8.1 to 67.142	8.098 to 66.374	8.1 to 66.498
Index ranges	$-7 \leq h \leq 6$, $-15 \leq k \leq 14$, $-19 \leq l \leq 18$	$-5 \leq h \leq 7$, $-14 \leq k \leq 12$, $-18 \leq l \leq 20$	$-7 \leq h \leq 7$, $-14 \leq k \leq 15$, $-15 \leq l \leq 19$
Reflections collected	7228	7179	7001
Independent reflections	2188 [$R_{\text{int}} = 0.0308$, $R_{\text{sigma}} = 0.0301$]	2158 [$R_{\text{int}} = 0.0230$, $R_{\text{sigma}} = 0.0236$]	2145 [$R_{\text{int}} = 0.0247$, $R_{\text{sigma}} = 0.0257$]
Data/restraints/parameters	2188/3/147	2158/3/147	2145/3/147
Goodness-of-fit on F^2	1.096	1.060	1.101
Final R indexes [$I \geq 2\sigma(I)$]	$R_1 = 0.0266$, $wR_2 = 0.0689$	$R_1 = 0.0230$, $wR_2 = 0.0570$	$R_1 = 0.0249$, $wR_2 = 0.0721$
Final R indexes [all data]	$R_1 = 0.0313$, $wR_2 = 0.0719$	$R_1 = 0.0269$, $wR_2 = 0.0594$	$R_1 = 0.0296$, $wR_2 = 0.0752$
Largest diff. peak/hole/ $e \text{ Å}^{-3}$	0.51/−0.49	0.54/−0.45	0.48/−0.45

3.3. Raman Spectrometry

The Raman spectrum of hydroxylclinohumite was recorded via Horiba Jobin–Yvon LabRam HR800 spectrometer using solid-state laser with $\lambda = 532$ nm (power on the sample 15 mW) and 100x objective. The sample was oriented randomly and measured at room temperature. The data were obtained in the range of 70–4000 cm^{-1} and 2 cm^{-1} spectral resolution. The calibration was carried out using Si standard (520.7 cm^{-1}).

4. Results

4.1. Major Element Mineral Chemistry

The SiO_2 , TiO_2 , MgO , FeO and F contents of the Luc Yen hydroxylclinohumite are similar to those reported in previous studies. The microprobe analysis yielded the averaged structural formula $(\text{Mg}_{0.69}\text{Ti}_{0.29}\text{Fe}_{0.02})_{\Sigma 1.00}\text{Mg}_{7.90}(\text{SiO}_4)_{\Sigma 4.09}[(\text{OH})_{1.10}\text{F}_{0.53}\text{O}_{0.37}]_{\Sigma 2.00}$, which is close to the ideal formula, $(\text{Mg}_{0.69}\text{Ti}_{0.29}\text{Fe}_{0.02})_{\Sigma 1.00}\text{Mg}_{8.00}(\text{SiO}_4)_{\Sigma 4.00}[(\text{OH})_{0.92}\text{F}_{0.50}\text{O}_{0.58}]_{\Sigma 2.00}$. The Mg# is lower in the Luc Yen hydroxylclinohumite than in others reported to date. The characteristic geochemical features of our hydroxylclinohumite are the high content of titanium, which attains 0.31 atoms per formula unit (3.94 wt.% TiO_2) and a low iron of 0.04 atoms per formula unit (0.41 wt.% FeO). The contents of Cl , Ca , and Mn are below the detection limits. The increased silicon content may be associated with microinclusions of humites with a ratio of forsterite and brucite layers greater than four [44,45].

4.2. Structure Description and Refinement

Both composition and crystal structure of humite group minerals are close to olivine. Their crystal structure is based on isolated silica-oxygen tetrahedrons $[\text{SiO}_4]$, connected with each other through Mg atoms. Forsterite layers (Mg_2SiO_4) are interspersed with $\text{Mg}(\text{OH},\text{F})_2$ layers; their ratio progressively changes from norbergite (1/1) to clinohumite (4/1). In general, the crystal structure of clinohumite is based on a hexagonal close-packed array (2H) of anions similar to that of forsterite (Figure 3a) [46]. As in the olivine structure type, in the structures of all humite minerals, 1/2 of the octahedral voids are occupied by the M cations while the occupancy of the available tetrahedral voids decreases from 1/8 in olivine over 1/9 in clinohumite ($n = 4$) to 1/12 in norbergite ($n = 1$) [47]. This structure can be also described as a heteropolyhedral framework consisting of stacking of identical sheets parallel to the (001) plane [48]. In turn, the sheets based on chains of edge-sharing $\text{Mg}1$ -5 octahedra are connected by vertex-shared $\text{Si}1$ -2 tetrahedra. The F ions and OH groups are located in the small cavities on the “missing” (compared with forsterite structure) SiO_4 tetrahedra (Figure 3b).

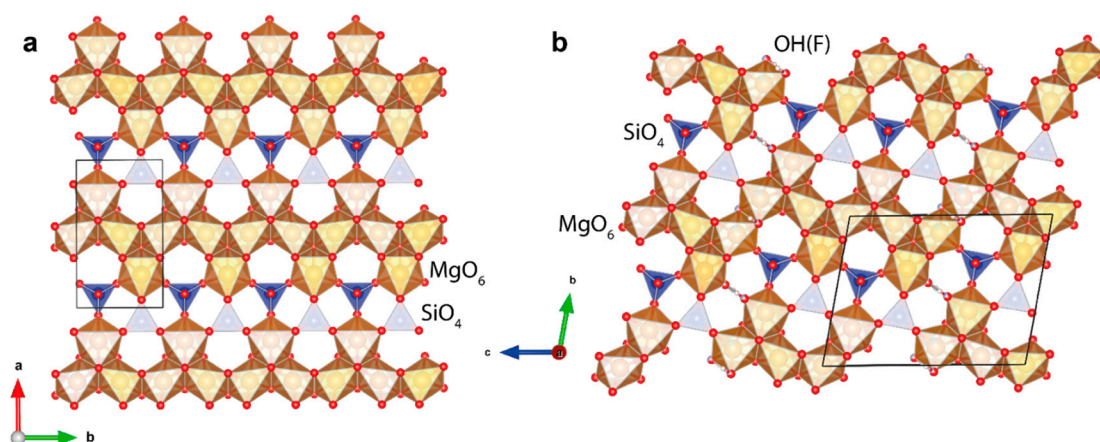


Figure 3. Heteropolyhedral sheet in the crystal structure of forsterite projected along c axis (a), the heteropolyhedral sheet in the crystal structure of hydroxylclinohumite (b). Legend: MgO_6 octahedra = brown, SiO_4 tetrahedra = blue, Mg, Si, O and H atoms are shown as orange, blue, red and pink spheres, respectively.

The crystal structure of hydroxylclinohumite contains five independent Mg sites. During refinement, the Mg5 site in all samples has negative values of the tensors and the corresponding atom described as non-positively defined (NPD) with numerous peaks of excess electron density $1 e^-$ within 0.5 \AA distance around the Mg5 site. The final refinements demonstrate an admixture of Ti at Mg5 site and the refined occupancies were $(\text{Mg}_{0.82}\text{Ti}_{0.18})$, $(\text{Mg}_{0.80}\text{Ti}_{0.20})$ and $(\text{Mg}_{0.78}\text{Ti}_{0.22})$ for samples V-11-2d, V-11-2a and V-12-03, respectively. Other Mg1-4 sites were refined as fully populated by Mg atoms.

The Si1-2 atoms has mean $\langle\text{Si-O}\rangle$ distances in the range $1.625\text{--}1.640 \text{ \AA}$ and populated by Si atoms only. The O9 atom in all structures has numerous peaks of electron density ($\sim 0.50 e^-$) within 0.5 \AA distance around site. According to previous data, the O9 site is populated by F in clinohumite [43], so the O9 site was refined with mixed occupancy of F. The final refinement occupancies for O9 site are $(\text{O}_{0.63}\text{F}_{0.37})$, $(\text{O}_{0.665}\text{F}_{0.335})$ and $(\text{O}_{0.68}\text{F}_{0.32})$ for samples V-11-2d, V-11-2a and V-12-03, respectively. Other O sites populated by O atoms only.

Position of the H atoms were found using Fourier difference synthesis ($F_o - F_{\text{calc}}$) around O9(F) site (Figure 4). Initially, two residual density ~ 0.30 (H10) and $0.50 e^-$ (H9) peaks within $0.90\text{--}1.00 \text{ \AA}$ distance from O9 site for the samples V-11-2d and V-11-2a, respectively, were found. Both sites were refined as H atoms; however Mg-H10 distance was $1.85\text{--}1.95 \text{ \AA}$, anomalously short to be real atom and excluded from the next refinement steps. For the V-12-03 sample only one peak of residual density near O9 site was observed. This peak corresponds to the position of H9 atoms. The occupancy of the H9 sites was fixed according the charge balance requirements.

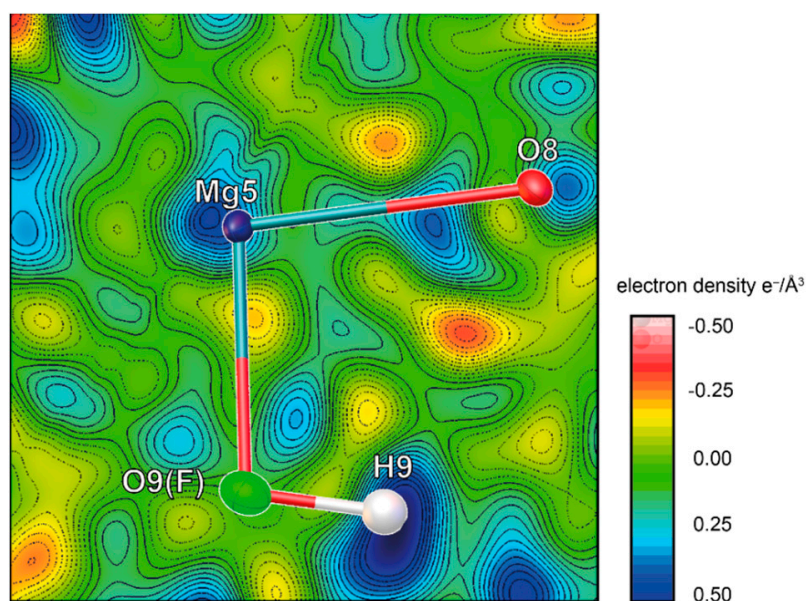


Figure 4. Fourier difference synthesis ($F_o - F_{\text{calc}}$) around O9(F) site in the crystal structure of V-12-03 sample. Projection is onto the $(0.137a, 0.403b, \text{ and } 0.535c)$ plane, contour intervals are $0.1 e^- / \text{\AA}^{-3}$.

The refined crystal chemical formula for the hydroxylclinohumite samples can be written as $(\text{Mg}_{8.82}\text{Ti}_{0.18})_{9.00}(\text{SiO}_4)_4[(\text{OH})_{0.90}\text{F}_{0.74}\text{O}_{0.36}]_{2.00}$ for the V-11-2d sample, $(\text{Mg}_{8.80}\text{Ti}_{0.20})_{9.00}(\text{SiO}_4)_4[(\text{OH})_{0.93}\text{F}_{0.67}\text{O}_{0.40}]_{2.00}$ for the V-11-2a sample and $(\text{Mg}_{8.78}\text{Ti}_{0.22})_{9.00}(\text{SiO}_4)_4[\text{OH}_{0.92}\text{F}_{0.64}\text{O}_{0.44}]_{2.00}$ for the V-12-03 sample, which agrees well with the empirical chemical data, considering close proximity between site-scattering powers of Ti and Fe. The discrepancy between refined predominance of hydroxide over fluorine compared to the electron microprobe analyses could result from measurement inaccuracy, matrix effect on EPMA analyses of fluorine [37], and/or minor chemical zonation. Considering all of these factors, the agreement between the structural and EPMA data is good. Additionally, the discrepancy between refined titanium content compared to the empirical formulae could result from the

possibility of small Ti content (and Fe) could be distributed among all five MgO₆ octahedra, but this cannot be supported by the structure refinement.

According to the SC XRD and powder neutron diffraction data, hydroxylclinohumite may contain two independent hydrogen sites [49,50]. In nature, hydroxylclinohumite which does not contain F and cations in Mg position is rare; more often Ti or Fe³⁺-containing species are found [51]. Incorporation of Ti⁴⁺ changes the positive cationic charge together with F admixture realized in the crystal structure of hydroxylclinohumite from the Luc Yen deposit, where OH do not exceed 1 *apfu*. According to our scheme of hydrogen bonds in hydroxylclinohumite (Figure 5), the $d_{O\cdots H}$ distances is in the range 2.007–2.034 Å. The estimated peaks according to Libowitzky correlation should be in the range 3510–3530 cm⁻¹ [52].

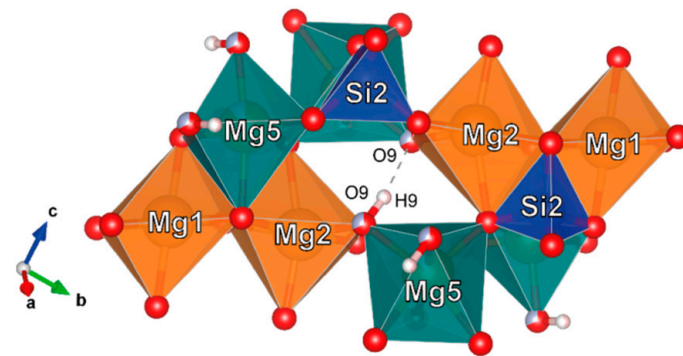


Figure 5. The local scheme of hydrogen bonding system of hydroxylclinohumite from the Luc Yen deposit.

4.3. Raman Spectroscopy

The Raman spectrum of hydroxylclinohumite from the Luc Yen deposit has the closest resemblance to the spectra of pure-Mg synthetic hydroxylclinohumite [53,54] and spectrum from the Luc Yen [36]. Spectra from [36] are presented with single crystal in two orientations. They illustrate strong polarization effect on the bands intensity. Our sample was randomly oriented and our spectrum is something average in orientation. It is also very similar to a natural hydroxylclinohumite from a marble-paragneiss unit of the Central Dabie medium-T/UHP eclogite-facies zone from the Ganjialing area, China [55] except some additional bands at 600–700 which Luc Yen hydroxylclinohumite lack probably due to very low Fe content.

Peaks positions (Figure 6a) are assigned according to Raman spectra reported in previous studies [53–55]: (1) the most intense bands 805, 827, 843, and 859 cm⁻¹ are corresponding to the stretching vibrations (ν_1) of the SiO₄ tetrahedra; (2) weak bands at 910, 929 and 964 cm⁻¹ are attributed to asymmetric stretching vibrations (ν_3) of the SiO₄ tetrahedra; (3) the bands of 744, 782 cm⁻¹ are ascribed to MgOH and TiOH deformations; (4) the bands at 550, 587, and 610 are corresponding to the out of plane (ν_4) bending modes of the SiO₄; (5) band at 430 cm⁻¹ is in plane (ν_2) bending mode of the SiO₄, and (6) the bands at 180, 230, 265, and 330 are due to the vibrations of the MgO₆ octahedra and the lattice vibrations. The most important peaks for hydroxylclinohumite in our spectrum are the ones which occur as two doublets at about 3389, 3406 cm⁻¹, 3556, and 3567 cm⁻¹ (Figure 6b) These bands in the OH-stretching region for the hydroxylclinohumite sample agree with those reported by Hurai et al. [36] who presented doublet 3339, and 3410 cm⁻¹ and triplet 3560, 3570, and 3578 cm⁻¹ and Liu et al. [53], who observed three strong bands at 3397, 3529 and 3564 cm⁻¹. The most intense band of stretching vibrations O–H at 3406 cm⁻¹ corresponds to strong hydrogen bonds OH \cdots O, which are formed between OH groups being at a relatively short distance from each other. The faint band at 3556 cm⁻¹ corresponds to the local situation, when the O(5) position, being an acceptor of the hydrogen bond, is occupied by F [56].

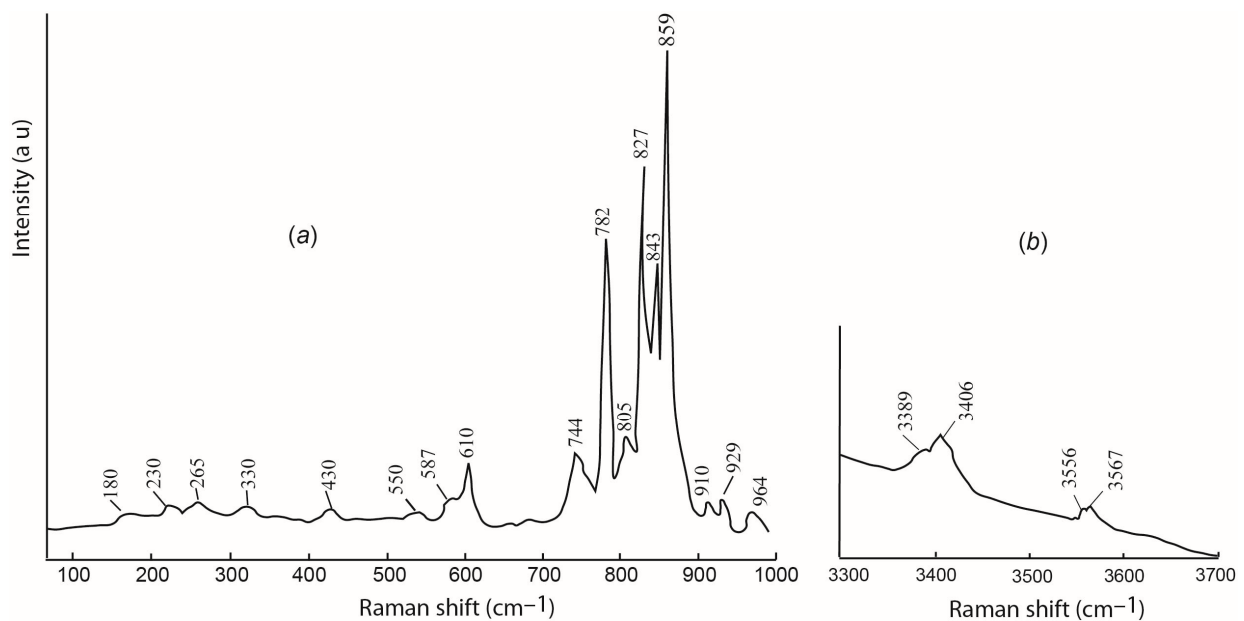


Figure 6. Raman spectra of hydroxylclinohumite specimen (V-11-2a) from the Luc Yen deposit: (a) bands are due to vibrations of the MgO_6 octahedra, the SiO_4 tetrahedra and the lattice vibrations; (b) the OH-stretching region.

5. Discussion

The rarity of hydroxylclinohumite in nature is mainly due to the behavior of CO_2 , H_2O and F in geochemical processes, the chemical composition of rocks and the physicochemical parameters of the mineral-forming medium.

The main minerals that characterize the most common associations with hydroxylclinohumite are dolomite, calcite, pargasite, forsterite, spinel, and corundum. As it was noted [57–59], formation of humite group minerals is facilitated by the presence of an aqueous fluid in the system. Therefore, petrogenesis of hydroxylclinohumite-bearing marble is considered further from the point of view of a metasomatic process, even if it was implemented locally.

As the model, we choose the Na–Mg–Al–Si– H_2O – CO_2 system, in terms of which, the most common original rocks of the protolith (evaporites, and terrigenous sediments) and the secondary minerals developed after them can be described satisfactorily. As it is known [58–60], the analysis of phase equilibria in the presence of a mixed H_2O – CO_2 fluid contributes to understanding the conditions of metamorphic transformations of siliceous dolomites. Let us consider the connection of chemical potentials of CO_2 and H_2O in a binary fluid ($\text{CO}_2 + \text{H}_2\text{O}$) at $p_{\text{CO}_2} + p_{\text{H}_2\text{O}} = p_{\text{total}} = \text{Const}$ and $T = \text{Const}$. Under these conditions, the values of the chemical potential of H_2O in the fluid ($\mu_{\text{H}_2\text{O}}$) are determined, as is known by the expression [39]:

$$\mu_{\text{H}_2\text{O}} = \mu_{\text{H}_2\text{O}}^0 + RT \ln f_{\text{H}_2\text{O}} = \mu_{\text{H}_2\text{O}}^0 + RT \ln \gamma_{\text{H}_2\text{O}} p_{\text{H}_2\text{O}} = \mu_{\text{H}_2\text{O}}^0 + RT \ln \gamma_{\text{H}_2\text{O}} (1 - x_{\text{CO}_2}) p_{\text{total}}$$

where, $\mu_{\text{H}_2\text{O}}^0$ is the standard chemical potential of water at a given temperature and pressure; $f_{\text{H}_2\text{O}}$, $\gamma_{\text{H}_2\text{O}}$, $p_{\text{H}_2\text{O}}$ is fugacity, fugacity coefficient and partial pressure of H_2O in the fluid, respectively; and x_{CO_2} is the molar fraction of CO_2 in the fluid.

To ascertain the main parameters of the mineral-forming medium that determine the stability of minerals in marble, consider the topology of diagrams constructed in the coordinates of chemical potentials [61]. The analysis of the model system is based on the fundamental principles of Korzhinsky [61,62]: there is a local equilibrium among minerals, all components have differential mobility, and incoming fluids react with protolith. This

approach has been successfully used to model the chemical transformation of metasomatic rocks [61].

The specific version of mineral associations with hydroxylclinohumite which can be formed in the system Na–Ca–Mg–Al–Si–H₂O–CO₂ depends on the chemical and mineral composition of the protolith.

In plotting the qualitative diagram ($\mu_{\text{CO}_2} - \mu_{\text{H}_2\text{O}}$) of the Na–Mg–Al–Si–CO₂–H₂O system for the transformations of forsterite and/or pargasite into hydroxylclinohumite, it is assumed that the pargasite of the Luc Yen deposit determines the main features of the chemical composition of amphibole in aluminum-rich pods in marble. Pargasite was found here in associations with dolomite, spinel, corundum, and hydroxylclinohumite. The mineral composition of the rocks was determined by the proportions of the Mg, Al and Si oxides, and the availability of sodium in the system determined by the presence of evaporites in the protolith [31,63] which leads to the formation of pargasite. Titanium oxide, which is present in the rocks in the form of ilmenite, titanite and rutile, can be considered a separate component. Lumping FeO and MgO together, we obtain three virtually inert components: (Mg, Fe)O, Al₂O₃, and SiO₂. CO₂ and H₂O are the main components producing the metamorphic transformation of the original rocks.

Thus, the number of phases in the model system is assumed to be six, and the number of inert components is three, leaving two completely mobile components. The temperature and pressure were taken as constant external equilibrium factors. The mineral equilibrium in such a system can be graphically depicted in a two-dimensional space. Therefore, we analyze in detail the behavior of the monovariant equilibrium reaction lines on the diagram in the coordinates of two fully mobile components ($\mu_{\text{CO}_2}, \mu_{\text{H}_2\text{O}}$).

The equations of the chemical reactions were calculated for the normative compositions of the minerals, the chemical composition of which is close to that of their natural analogs (Table 3). The equations are given in Table 4. Figure 7 presents this diagram in its entirety. It should be noted that three reactions 7, 9, and 12 (Table 4) are omitted in Figure 7 because nonvariant points [Hchu], [Crn] and [Fo] are metastable.

Table 3. Crystallochemical formulas of minerals (end members of solid-solution) adopted for calculating chemical reaction equations.

Mineral	Symbol	Formula	Mg	Al	Si
Hydroxylclinohumite	Hchu	Mg ₉ (SiO ₄) ₄ (OH) ₂	9	0	4
Pargasite	Prg	NaCa ₂ (Mg ₄ Al) _{Σ5} (Al ₂ Si ₆ O ₂₂)(OH) ₂	4	3	6
Forsterite	Fo	Mg ₂ SiO ₄	2	0	1
Dolomite	Dol	CaMg(CO ₃) ₂	1	0	0
Spinel	Spl	MgAl ₂ O ₄	1	2	0
Corundum	Crn	Al ₂ O ₃	0	2	0

The formation of hydroxylclinohumite in this system is controlled by three reactions (5, 4, and 14, blue solid line on Figure 7), by which it is completely destroyed when $\mu_{\text{H}_2\text{O}}$ decreases. Monovariant singular equilibria of the reactions 1–3 (Table 4) are controlled only by the chemical potential of CO₂ in the fluid and do not depend on the activity of water in the medium. Thus, in case of increasing μ_{CO_2} (and x_{CO_2}), spinel is replaced by an association of corundum+dolomite according to reactions 2 and 3 (red solid line on Figure 7). This monovariant line divides the diagram into two parts (Figure 7). In the upper part, only corundum is stable in association with forsterite, pargasite and dolomite (fields I, and II), and with increasing water activity, corundum associated with hydroxylclinohumite which replace forsterite and pargasite (fields III, VII, and VIII).

It follows from the diagram that at low activities of CO₂ and H₂O (below red solid line), spinel is stable with forsterite in excess of dolomite (field IV) and with an increase in aluminum content corundum+ spinel associations are possible. With increasing $\mu_{\text{H}_2\text{O}}$, hydroxylclinohumite is stable in association with spinel and corundum (fields V, VI, IX, X, and XI) at low activities of CO₂ (below red solid line).

Table 4. Equations of chemical reactions occurring on lines of monovariant equilibrium.

N	Symbols *	Chemical Reactions
1	[PrgDol]	$4\text{Fo} + \text{Spl} + \text{H}_2\text{O} = \text{Hchu} + \text{Crn}$
2	[PrgHchu]	$\text{Dol} + \text{Crn} = \text{Spl} + (\text{Cal}) + \text{CO}_2$
3	[PrgFo]	$\text{Dol} + \text{Crn} = \text{Spl} + (\text{Cal}) + \text{CO}_2$
4	[PrgSpl]	$\text{Dol} + 4\text{Fo} + \text{H}_2\text{O} = \text{Hchu} + (\text{Cal}) + \text{CO}_2$
5	[PrgCrn]	$\text{Dol} + 4\text{Fo} + \text{H}_2\text{O} = \text{Hchu} + (\text{Cal}) + \text{CO}_2$
6	[FoDol]	$3\text{Hchu} + 22\text{Crn} + 4(\text{Cal}) + 2\text{Na}^+ = 2\text{Prg} + 19\text{Spl} + 4\text{CO}_2 + 2\text{H}^+$
7	[FoHchU]	$\text{Dol} + \text{Crn} = \text{Spl} + (\text{Cal}) + \text{CO}_2$
8	[FoSpl]	$19\text{Dol} + 2\text{Prg} + 2\text{H}^+ = 3\text{Hchu} + 3\text{Crn} + 23(\text{Cal}) + 15\text{CO}_2 + 2\text{Na}^+$
9	[FoCrn]	$22\text{Dol} + 2\text{Prg} + 2\text{H}^+ = 3\text{Hchu} + 3\text{Spl} + 26(\text{Cal}) + 18\text{CO}_2 + 2\text{Na}^+$
10	[HchuDol]	$2\text{Prg} + 16\text{Spl} + 4\text{CO}_2 + 2\text{H}^+ = 12\text{Fo} + 19\text{Crn} + 4(\text{Cal}) + 3\text{H}_2\text{O} + 2\text{Na}^+$
11	[HchuSpl]	$2\text{Prg} + 16\text{Dol} + 2\text{H}^+ = 12\text{Fo} + 3\text{Crn} + 20(\text{Cal}) + 3\text{H}_2\text{O} + 12\text{CO}_2 + 2\text{Na}^+$
12	[HchuCrn]	$2\text{Prg} + 19\text{Dol} + 2\text{H}^+ = 12\text{Fo} + 3\text{Spl} + 23(\text{Cal}) + 2\text{H}_2\text{O} + 15\text{CO}_2 + 2\text{Na}^+$
13	[SplDol]	$76\text{Fo} + 3\text{Crn} + 4(\text{Cal}) + 19\text{H}_2\text{O} + 2\text{Na}^+ = 16\text{Hchu} + 2\text{Prg} + 2\text{H}^+ + 4\text{CO}_2$
14	[SplCrn]	$\text{Hchu} + (\text{Cal}) + \text{CO}_2 = 4\text{Fo} + \text{Dol} + 2\text{H}_2\text{O}$
15	[DolCrn]	$88\text{Fo} + 3\text{Spl} + 4(\text{Cal}) + 22\text{H}_2\text{O} + 2\text{Na}^+ = 19\text{Hchu} + 2\text{Prg} + 4\text{CO}_2 + 2\text{H}^+$

* Reactions are indicated by symbols of minerals not involved in the reaction: ([PrgDol] = "Prg and Dol"- absent in the reaction).

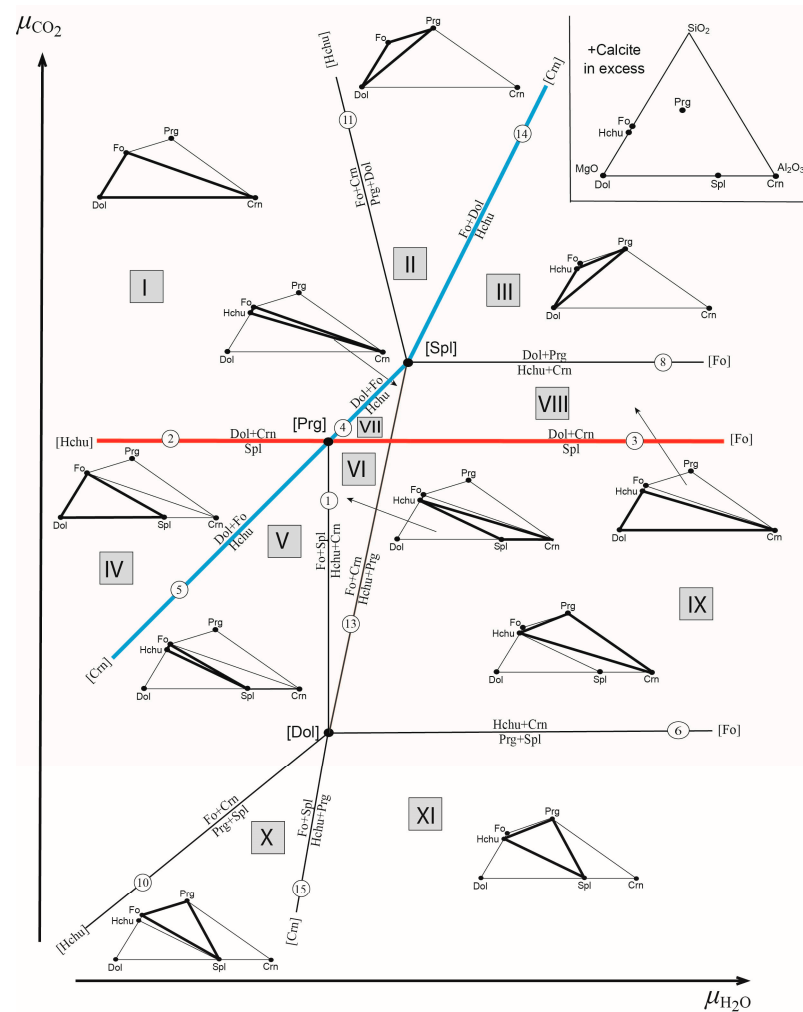


Figure 7. Qualitative $\mu_{\text{CO}_2} - \mu_{\text{H}_2\text{O}}$ diagram of mineral parageneses of hydroxylclinohumite in the system Na-Mg-Al-Si-CO₂-H₂O. I, . . . ,XI are stable divariant fields; the numbers in circles indicate the reaction numbers in Table 4. Bold lines in triangles highlight characteristic parageneses that are stable only in this field of the diagram, which follows from the equations of monovariant reactions that limit each field.

Thus, the two-dimensional diagram clearly illustrates the stability of the main minerals in marble (dolomite±calcite in all parageneses) depending on the chemical potentials of H₂O and CO₂ in the mineral-forming medium.

The rarity of hydroxylclinohumite in marbles seems to be due to unusual chemical compositions of protolith and fluid: clinogumite–fluid partition coefficient's of fluorine are always greater than unity, with average coefficients of $D_F^{\text{chu/fluid}} \approx 3$ [8].

The fact that hydroxylclinohumite overgrows partially broken and fractured spinel grains indicates its crystallization after the gem spinel formation probably due to dehydration of serpentine or breakdown of forsterite [15].

Experiments have proven clinohumite's stability ranging between ~700° and 1100 °C and P between 29 and 77 kb [64], however, the presence of Ti and F makes it stable under certain P-T condition in the mantle. These temperatures are consistent with previous estimates of about 700 °C minimum temperature for the formation of the Luc Yen spinel [65].

6. Conclusions

Hydroxylclinohumite is known as an accessory phase in a wide variety of ultrabasic and carbonate rocks of high-pressure origin. The first occurrence of titanian hydroxylclinohumite in pods of gem spinel hosted marbles of the Luc Yen deposit, northern Vietnam is reported. In marbles, besides calcite and dolomite, it also associates with spinel, forsterite and pargasite. The article presents the complete chemical, structural and spectroscopic characteristics of hydroxylclinohumite.

The average composition of hydroxylclinohumite of the Luc Yen deposit is $(\text{Mg}_{0.69}\text{Ti}_{0.29}\text{Fe}_{0.02})_{\Sigma 1.00}\text{Mg}_{7.91}(\text{SiO}_4)_{4.08}[(\text{OH})_{1.10}\text{F}_{0.53}\text{O}_{0.37}]_{\Sigma 2.00}$. A characteristic geochemical feature of the studied hydroxylclinohumite is a reduced iron content, which reaches 0.04 atoms per formula unit (0.42 wt.% FeO).

In addition to data on element substitutions and the crystal structure, we describe the conditions for the formation of hydroxylclinohumite in the deposit. It follows from the clinogumite–fluid partition coefficient's of fluorine ($D_F^{\text{chu/fluid}} \approx 3$) that the formation of hydroxylclinohumite requires that the activity (concentration) of H₂O in solution is approximately three times higher than the activity of fluorine.

Additionally, we incline to the conclusion that such middle-T/HP metamorphism favors crystallization of hydroxylclinohumite in marbles together or after with gem spinel formation in a subducting slab.

Supplementary Materials: The following supporting information can be downloaded at: <https://www.mdpi.com/article/10.3390/min13070901/s1>, Table S1. Fractional atomic coordinates and equivalent isotropic displacement parameters (Å²) for hydroxylclinohumite V-11-2d sample; Table S2. Selected interatomic distances for hydroxylclinohumite V-11-2d sample; Table S3. Fractional atomic coordinates and equivalent isotropic displacement parameters (Å²) for hydroxylclinohumite V-11-2a sample; Table S4. Selected interatomic distances for hydroxylclinohumite V-11-2a sample; Table S5. Fractional atomic coordinates and equivalent isotropic displacement parameters (Å²) for hydroxylclinohumite V-12-03 sample; Table S6. Selected interatomic distances for hydroxylclinohumite V-12-03 sample.

Author Contributions: Conceptualization, V.G.K. and P.B.S.; methodology, V.G.K., P.B.S. and K.A.K.; validation, V.G.K. and P.B.S.; investigation, K.A.K., T.L.P., V.N.B. and G.A.G.; Please list all the tables here along their titles and ensure they are cited in the main text—writing—original draft preparation, V.G.K., K.A.K. and T.L.P.; writing—review and editing, V.G.K., K.A.K. and P.B.S.; visualization, V.G.K. and K.A.K.; supervision, V.G.K. and P.B.S.; funding acquisition, P.B.S. and V.G.K. All authors have read and agreed to the published version of the manuscript.

Funding: The studies were supported by the Russian Science Foundation, grant no. 22-27-00172.

Data Availability Statement: The data presented in this study are available upon request from the corresponding author.

Acknowledgments: We are grateful to three anonymous reviewers for their constructive and insightful reviews of the manuscript. The X-ray diffraction measurements were performed in the Centre for the Collective Use of Equipment of Kola Science Centre, Russian Academy of Sciences. The microprobe analysis and Raman spectrum were obtained in the Geomodel Center at St. Petersburg University.

Conflicts of Interest: The authors declare no conflict of interest.

References

1. McGetchin, T.R.; Silver, L.T.; Chodos, A.A. Titanoclinohumite: A possible mineralogical site for water in the upper mantle. *J. Geophys. Res.* **1970**, *75*, 244–259. [\[CrossRef\]](#)
2. Aoki, K.; Fujino, K.; Akaogi, M. Titanochondrodite and titanoclinohumite derived from the upper mantle in the Buell Park kimberlite, Arizona, USA. *Contrib. Miner. Petrol.* **1976**, *56*, 243–254. [\[CrossRef\]](#)
3. Papike, J.; Cameron, M. Crystal chemistry of silicate minerals of geophysical interest. *Rev. Geophys. Sp. Phys.* **1976**, *14*, 37–80. [\[CrossRef\]](#)
4. Kanzaki, M. Stability of hydrous magnesium silicates in the mantle transition zone. *Phys. Earth Plan. Inter.* **1991**, *66*, 307–312. [\[CrossRef\]](#)
5. Wunder, B.; Medenbach, O.; Daniels, P.; Schreyer, W. First synthesis of the hydroxyl end-member of humite, $Mg_7Si_3O_{12}(OH)_2$. *Amer. Miner.* **1995**, *80*, 638–640.
6. Zheng, Y.F. Metamorphic chemical geodynamics in continental subduction zones. *Chem. Geol.* **2012**, *328*, 5–48. [\[CrossRef\]](#)
7. Arai, S.; Ishimaru, S.; Mizukami, T. Methane and propane micro-inclusions in olivine in titanoclinohumite-bearing dunites from the Sanbagawa high-P metamorphic belt, Japan: Hydrocarbon activity in a subduction zone and Ti mobility. *Earth Planet. Sci. Lett.* **2012**, *353*, 1–11. [\[CrossRef\]](#)
8. Hughes, L.; Pawley, A. Fluorine partitioning between humite-group minerals and aqueous fluids: Implications for volatile storage in the upper mantle. *Contrib. Miner. Petrol.* **2019**, *174*, 78. [\[CrossRef\]](#)
9. Gekimiyants, V.M.; Sokolova, E.V.; Spiridonov, E.M.; Ferraris, G.; Chukanov, N.V.; Prencipe, M.; Avdonin, V.N.; Polenov, Y.A. Hydroxylclinohumite $Mg_9(SiO_4)_4(OH,F)_2$ -a new mineral of the humite group. *Zapiski RMO.* **1999**, *128*, 64–70. (In Russian)
10. Borneman-Starynkevich, I.D.; Myasnikov, V.S. On isomorphic substitution in Clinohumite. *Compt. Rend. Acad. Sci. URSS* **1950**, *71*, 137–140. (In Russian)
11. Beeker, P. Klinohumite vom Laperwitzbach, Dorfertal, Osttirol. *Karinthin* **1976**, *75*, 257–260. (In German)
12. Mitchell, R.H. Manganous magnesian ilmenite and titanian clinohumite from the Jacupiranga carbonatite, Sao Paulo, Brazil. *Amer. Miner.* **1978**, *63*, 544–547.
13. Möckel, J.R. Structural petrology of the garnet peridotite of Alpe Arami (Ticino), Switzerland. *Leid. Geol. Med.* **1969**, *42*, 61–130.
14. Trommsdorff, V.; Evans, B.W. Titanian hydroxyl-clinohumite formation and breakdown in antigorite rocks (Malenco-Italy). *Contrib. Miner. Petrol.* **1980**, *72*, 229–242. [\[CrossRef\]](#)
15. Ehlers, K.; Hoinkes, G. Titanian Chondrodite and Clinohumite in Marbles from the Ötztal Crystalline Basement. *Miner. Petrol.* **1987**, *36*, 13–25. [\[CrossRef\]](#)
16. Jones, N.W.; Ribbe, P.H.; Gibbs, G.V. Crystal chemistry of the humite minerals. *Amer. Miner.* **1969**, *54*, 391–411.
17. Fujino, K.; Takeuchi, Y. Crystal chemistry of titanian chondrodite and titanian clinohumite of high pressure origin. *Amer. Miner.* **1978**, *63*, 535–543.
18. Ribbe, P.H. Titanium, fluorine and hydroxyl in humite minerals. *Amer. Miner.* **1979**, *64*, 1027–1035.
19. Huong, L.T.-T.; Haeger, T.; Phan, T.-L. Study of impurity in blue spinel from the Luc Yen mining area, Yen Bai province, Vietnam. *Vietnam J. Earth Sci.* **2018**, *40*, 47–55. [\[CrossRef\]](#)
20. Chauvire, B.; Rondeau, B.; Fritsch, E.; Ressigeac, P.; Devidal, J.-L. Blue spinel from the Luc Yen district of Vietnam. *Gems Gemol.* **2015**, *51*, 2–17. [\[CrossRef\]](#)
21. Huong, L.T.-T.; Häger, T.; Hofmeister, W.; Hauzenberger, C.; Schwarz, D.; Long, P.V.; Wehrmeister, W.; Khoi, N.N.; Nhung, N.T. Gemstones from Vietnam: An update. *Gems Gemol.* **2012**, *48*, 158–176. [\[CrossRef\]](#)
22. Sokolov, P.; Kuksa, K.; Marakhovskaya, O.; Gussias, G.A. In search of cobalt blue spinel in Vietnam. *Color Summer* **2019**, *43*, 43–49.
23. Peretti, A.; Günther, D. Spinel from Namya. *Contrib. Gem.* **2003**, *2*, 15–18.
24. Malsy, A.-K.; Klemm, L. Distinction of gem spinels from the Himalayan mountain belt. *Chim. Int. J. Chem.* **2010**, *64*, 741–746. [\[CrossRef\]](#)
25. Sutthirat, C.; Lapngamchana, S.; Pisutha-Arnond, V.; Khoi, N.N. Petrography and some mineral chemistry of gem-bearing marble from Luc Yen deposit, northern Vietnam. In Proceedings of the International Symposia on Geoscience Resources and Environments of Asian Terranes (GREAT 2008), Bangkok, Thailand, 24–26 November 2008; pp. 283–288.
26. Häger, T.; Hauzenberger, C.; Lehmann, C.; Zimmer, D.; Nguyen Ngoc Khoi, D.A.T.; Le Thi-Thu Huong, H.W. Causes of colour of natural untreated spinels from Vietnam in comparison to flame fusion and flux grown synthetics. In Proceedings of the 33rd International Gemmological Conference, Hanoi, Vietnam, 10 October 2013; pp. 89–91.
27. Garnier, V.; Ohnenstetter, D.; Giuliani, G.; Maluski, H.; Deloule, E.; Phan Trong, T.; Pham Van, L.; Hoàng Quang, V. Age and significance of ruby-bearing marble from the Red River Shear Zone, northern Vietnam. *Can. Miner.* **2005**, *43*, 1315–1329. [\[CrossRef\]](#)

28. Garnier, V.; Giuliani, G.; Ohnenstetter, D.; Fallick, A.E.; Dubessy, J.; Banks, D.; Vinh, H.Q.; Lhomme, T.; Maluski, H.; Pêcher, A. Marble-hosted ruby deposits from central and southeast Asia: Towards a new genetic model. *Ore Geol. Rev.* **2008**, *34*, 169–191. [[CrossRef](#)]
29. Giuliani, G.; Fallick, A.E.; Boyce, A.J.; Pardieu, V.; Pham, V.L. Pink and red spinels in marble: Trace elements, oxygen isotopes, and sources. *Can. Miner.* **2017**, *55*, 743–761. [[CrossRef](#)]
30. Fallick, A.E.; Giuliani, G.; Rigaudier, T.; Boyce, A.J.; Pham, V.L.; Pardieu, V. Remarkably uniform oxygen isotope systematics for co-existing pairs of gem-spinel and calcite in marble, with special reference to Vietnamese deposits. *Comp. Rend. Geosci.* **2019**, *351*, 27–36. [[CrossRef](#)]
31. Krivovichev, V.G.; Kuksa, K.A.; Sokolov, P.B.; Marakhovskaya, O.Y.; Klimacheva, M.E. Marble-hosted noble spinel deposits from Luc Yen district (Vietnam): Mineral systems and some aspects of genesis. *Zapiski RMO.* **2022**, *147*, 37–49. (In Russian)
32. Hofmeister, A.; Mao, H. Evaluation of shear moduli and other properties of silicates with the spinel structure from IR spectroscopy. *Amer. Miner.* **2001**, *86*, 622–639. [[CrossRef](#)]
33. Kuksa, K.; Sokolov, P.; Marakhovskaya, O.; Gussias, G.; Brownscombe, W. Mineralogy, geochemistry and genesis of the Luc Yen noble spinel deposit, Vietnam. *Mineralogy* **2019**, *5*, 56–69. (In Russian) [[CrossRef](#)]
34. Long, P.V.; Giuliani, G. Update on gemstone mining in Luc Yen, Vietnam. *Gems Gemol.* **2013**, *49*, 31–46. [[CrossRef](#)]
35. Hauzenberger, C.A.; Häger, T.; Hofmeister, W.; Quang, V.X.; Rohan Fernando, G.W.A. Origin and formation of gem quality corundum from Vietnam. In Proceedings of the International Workshop, “Geo- and Material-Science on Gem-Minerals of Vietnam”, Hanoi, Vietnam, 1–8 October 2003; pp. 1–8.
36. Hurai, V.; Wierzbicka-Wieczorek, M.; Pentrák, M.; Huraiová, M.; Thomas, R.; Swierczewska, A.; Luptáková, J. X-ray Diffraction and Vibrational Spectroscopic Characteristics of Hydroxylclinohumite from Ruby-Bearing Marbles (Luc Yen District, Vietnam). *Intern. J. Miner.* **2014**, *2014*, 648530. [[CrossRef](#)]
37. Ottolini, L.; C’amara, F.; Bigi, S. An investigation of matrix effects in the analysis of fluorine in humite-group minerals by EMPA, SIMS, and SREF. *Amer. Miner.* **2000**, *85*, 89–102. [[CrossRef](#)]
38. Long, P.V.; Giuliani, G.; Fallick, A.E.; Boyce, A.J.; Pardieu, V. Trace elements and oxygen isotopes of gem spinels in marble from the Luc Yen-An Phu areas, Yen Bai province, North Vietnam. *Vietnam J. Earth Sci.* **2018**, *40*, 165–177. [[CrossRef](#)]
39. Krivovichev, V.G.; Kuksa, K.A.; Sokolov, P.B.; Marakhovskaya, O.Y.; Zolotarev, A.A.; Bocharov, V.N.; Semenova, T.F.; Klimacheva, M.E.; Gussiás, G.A. Preiswerkite: A First Occurrence in Marble Hosting Gem Spinel Deposits, Luc Yen, Vietnam. *Minerals* **2022**, *12*, 1024. [[CrossRef](#)]
40. *Agilent Technologies CrysAlis CCD and CrysAlis RED*; Oxford Diffraction Ltd.: Yarnton, UK, 2014.
41. Sheldrick, G.M. Crystal structure refinement with SHELXL. *Acta Crystallogr. Sect. C Str. Chem.* **2015**, *71*, 3–8. [[CrossRef](#)]
42. Izumi, F.; Momma, K. Three-Dimensional Visualization in Powder Diffraction. *Solid State Phen.* **2007**, *130*, 15–20. [[CrossRef](#)]
43. Robinson, K.; Gibbs, G.V.; Ribbe, P.H. The crystal structures of the humite minerals. IV. Clinohumite and titanoclinohumite. *Amer. Miner.* **1973**, *58*, 43–49.
44. White, T.J.; Hyde, B.G. Electron microscope study of the humite minerals: I Mg-rich specimens. *Phys. Chem. Minerals* **1982**, *8*, 55–63. [[CrossRef](#)]
45. Gaspar, J.C. Titanian clinohumite in the carbonatites of the Jacupiranga Complex, Brazil: Mineral chemistry and comparison with titanian clinohumite from other environments. *Amer. Miner.* **1992**, *77*, 168–178.
46. Bragg, W.L.; West, J. The structure of certain silicates. *Proc. R. Soc. London. Ser. A* **1927**, *114*, 450–473. [[CrossRef](#)]
47. Langer, K.; Platonov, A.N.; Matsyuk, S.; Wildner, M. The crystal chemistry of the humite minerals: Fe²⁺-Ti⁴⁺ charge transfer and structural allocation of Ti⁴⁺ in chondrodite and clinohumite. *Eur. J. Miner.* **2002**, *14*, 1027–1032. [[CrossRef](#)]
48. Mikhailova, J.A.; Ivanyuk, G.Y.; Kalashnikov, A.O.; Pakhomovsky, Y.A.; Bazai, A.V.; Panikorovskii, T.L.; Yakovenchuk, V.N.; Konoplev, N.G.; Goryainov, P.M. Three-D mineralogical mapping of the kovdor phoscorite-carbonatite complex, NW Russia: I. Forsterite. *Minerals* **2018**, *8*, 260. [[CrossRef](#)]
49. Friedrich, A.; Lager, G.A.; Kunz, M.; Chakoumakos, B.C.; Smyth, J.R.; Schultz, A.J. Temperature-dependent single-crystal neutron diffraction study of natural chondrodite and clinohumites. *Amer. Miner.* **2001**, *86*, 981–989. [[CrossRef](#)]
50. Berry, A.J.; James, M. Refinement of hydrogen positions in synthetic hydroxyl-clinohumite by powder neutron diffraction. *Amer. Miner.* **2001**, *86*, 181–184. [[CrossRef](#)]
51. Ferraris, G.; Prencipe, M.; Sokolova, E.; Gekimyants, V.M.; Spiridonov, E.M. Hydroxylclinohumite, a new member of the humite group: Twinning, crystal structure and crystal chemistry of the clinohumite subgroup. *Zeitschrift für Krist.-Cryst. Mater.* **2000**, *215*, 169–173. [[CrossRef](#)]
52. Libowitzky, E. Correlation of O-H Stretching Frequencies and O-H . . . O Hydrogen Bond Lengths in Minerals. *Hydrog. Bond Res.* **1999**, *1059*, 103–115. [[CrossRef](#)]
53. Liu, D.; Pang, Y.; Ye, Y.; Jin, Z.; Smyth, J.R.; Yang, Y.; Zhang, Z.; Wang, Z. In-situ high-temperature vibrational spectra for synthetic and natural clinohumite: Implications for dense hydrous magnesium silicates in subduction zones. *Amer. Miner.* **2019**, *104*, 53–63. [[CrossRef](#)]
54. Frost, R.; Palmer, S.; Bouzaid, J.; Reddy, J. A Raman spectroscopic study of humite minerals. *J. Raman Spectr.* **2007**, *38*, 68–77. [[CrossRef](#)]
55. Ye, Y.; Smyth, J.R.; Jacobsen, S.D.; Goujon, C. Crystal chemistry, thermal expansion, and Raman spectra of hydroxyl-clinohumite: Implications for water in Earth’s interior. *Contrib. Miner. Petrol.* **2013**, *165*, 563–574. [[CrossRef](#)]

56. Pekov, I.V.; Gerasimova, E.I.; Chukanov, N.V.; Kabalov, Y.K.; Zubkova, N.V.; Zadov, A.E.; Yapaskurt, V.O.; Gekimyants, V.M.; Pushcharovskii, D.Y. Hydroxylchondrodite $Mg_5(SiO_4)_2(OH)_2$: A new mineral of the humite group and its crystal structure. *Doklady Earth Sciences* **2011**, *436*, 230–236. [[CrossRef](#)]
57. Duffy, C.J.; Greenwood, H.J. Phase equilibria in the system MgO-MgF₂-SiO₂-H₂O. *Amer. Miner.* **1979**, *64*, 1156–1174.
58. Rice, J.M. Phase equilibria involving humite minerals in impure dolomitic limestones: Part I. Calculated stability of clinohumite. *Contrib. Miner. Petrol.* **1980**, *71*, 219–235. [[CrossRef](#)]
59. Bucher, K.; Rodney, G. *Petrogenesis of Metamorphic Rocks*, 8th ed.; Springer: Berlin/Heidelberg, Germany, 2011; p. 428. [[CrossRef](#)]
60. Spear, F.S. *Metamorphic Phase Equilibria and Pressure-Temperature-Time Paths*; Mineralogical Society of America: Washington, IL, USA, 1995; p. 799.
61. Korzhinskiy, D.S. *Physico-Chemical Basis of the Analysis of the Paragenesis of Minerals*; Consultants Bureau, New York and Chapman & Hall: London, UK, 1959; p. 142.
62. Korzhinskiy, D.S. *Teoreticheskiye Osnovy Analiza Paragenезisov Mineralov (Theoretical Basis of Analysis of Mineral Para-Geneses)*; Nauka: Moscow, Russia, 1973; p. 288.
63. Giuliani, G.; Dubessy, J.; Ohnenstetter, D.; Banks, D.; Branquet, Y.; Feneyrol, J.; Fallick, A.E.; Martelat, J.-E. The role of evaporites in the formation of gems during metamorphism of carbonate platforms: A review. *Miner. Deposita* **2018**, *53*, 1–20. [[CrossRef](#)]
64. Yamamoto, K.; Akimoto, S. The system MgO-SiO₂-H₂O at high pressures and temperatures-stability field for hydroxylchondrodite, hydroxyl-clinohumite and 10 A-phase. *Amer. J. Sci.* **1977**, *277*, 288–312. [[CrossRef](#)]
65. Hauzenberger, C.A.; Häger, T.; Baumgartner, L.P.; Hofmeister, W. High-grade metamorphism and stable-isotope geochemistry of N-Vietnamese gem-bearing rocks. In *Material Characterization by Solid State Spectroscopy: Gems and Mineral of Vietnam*; Hofmeister, W., Dao, N.Q., Quang, V.X., Eds.; International Workshop: Hanoi, Vietnam, 2001; pp. 124–138.

Disclaimer/Publisher’s Note: The statements, opinions and data contained in all publications are solely those of the individual author(s) and contributor(s) and not of MDPI and/or the editor(s). MDPI and/or the editor(s) disclaim responsibility for any injury to people or property resulting from any ideas, methods, instructions or products referred to in the content.